8

UPPER ATMOSPHERE STUDIES

The Earth's atmosphere occupies some million times greater volume than the solid Earth. In this huge system, the charged plasma particles react strongly to electric and magnetic fields. Hence, electrical processes in one part of the system can influence the electrodynamical processes in another distant part. The redistribution of the charged particles in turn can modify the existing electric and magnetic fields in the atmosphere. Hence, an investigation of electrodynamical processes in various regions of the atmosphere and their coupling is very important for understanding the state of electrical environment of the Earth's atmosphere.

The region-wise electrodynamical study of the Earth's atmosphere is not feasible. The electric fields and currents do not care for human-designated boundaries such as tropopause, stratopause, mesospause and ionosphere. They propagate from one region to another and affect the entire electrodynamical processes, hence cannot be studied in isolation. An integrated approach using satellites and modern sophisticated instruments is required to advance the knowledge about dynamics of the near-Earth environment. This approach provides a framework for exploring interconnections and coupling of various regions and also for explaining the solar-terrestrial-weather relationships. Some of the important findings over the past few decades are reported in this chapter.

Little is known about the need for Earth to generate a large scale magnetic field to shield it from the high-energy radiation and wind from the Sun. However, it is now well known without the magnetic field, the atmosphere would be exposed to ionization and erosion by the charged particles in the solar wind. Thus, any form of early life would have been irradiated by the intense X-ray and high-energy UV emission from the Sun (Fig. 8.1a). The principal components of geomagnetic variations recorded by ground observations are due to currents and fields in the near-Earth space starting from ~80 km from the surface to the magnetopause and beyond. These are even intimately related to the electric fields at much lower heights, where meteorological features

N. Basavaiah, *Geomagnetism*

predominate. Thus, the purpose of upper atmosphere studies is to address the phenomena occurring in the ionosphere, magnetosphere and beyond.

The Earth's atmosphere extends up to the magnetopause, which acts as a boundary between the Earth and the interplanetary medium and between the solar wind and the magnetosphere (Fig. 8.1b). Here, the solar wind dynamic pressure is balanced by the geomagnetic field pressure. The EMF is more or less confined inside the magnetopause boundary. A schematic of the 2D view of the magnetosphere (Fig. 8.1b) is correlated to 3D (Fig. 8.1c), which is the view obtained by an observer from outside the magnetosphere. It shows various important plasma regions, current systems and several effects due to the interaction of the solar wind with the EMF. The EMF is pushed back by high pressure solar wind into a characteristic shape known as the magnetosphere (Chapter 3). A bow shock is formed ~3-4 R_E ahead of the magnetopause, a boundary inside which EMF is contained because of solar wind pressure. Some particles of solar wind are captured by the EMF and are forced into a system of radiation belts called Van Allen radiation belts that girdle the Earth. Other familiar geomagnetic phenomena such as polar auroras and the communication disrupting ionospheric disturbances associated with magnetic storms arise due to the complex interplay between the solar wind and the Earth's atmosphere (Fig. 8.1a). Studies bear out that the radiation of Van Allen is highest over the geomagnetic equator and diminishes towards the poles. Auroras occur most frequently in concentric rings around the geomagnetic poles and diminish in frequency towards the equator.

In recent times, there has been keen interest in understanding Sun-Earth connection events. Magnetic storms are perhaps important components of space weather effects on Earth (Fig. 8.1). Super-intense magnetic storms have the largest societal and technological relevance, causing life-threatening power outages, satellite damages, communication failures and navigational problems. Thus, research on historical geomagnetic storms aids to create a good database of preceding and imminent intense and super-intense magnetic storms. Such study is carried to answer some basic questions: (1) how many super-intense magnetic storms have occurred in the last 160 years and what were their probable solar and interplanetary causes? (2) frequency of occurrence of super-intense storms and under what circumstances? (3) is a prediction of certain number (say 3) most severe magnetic storm during a solar cycle possible? (4) can the possible damaging effect of super-intense magnetic storms on the modern society be predicted in advance? and (5) what is the energetic effect of eruptive phenomena on Sun and Stars. The correlations between selective features on the Sun and surface magnetic field changes enable to predict the possibility of the occurrence of violent geomagnetic disturbances.

The investigation of various processes in Earth's magnetosphere responsible for the generation of large scale electric field with the focus on magnetic reconnection at the magnetopause and in the tail region is carried out analytically as well as numerically. The study advances the knowledge about magnetic

reconnection, a basic plasma physics process, which converts magnetic energy into the plasma heat and flow energy. Generation of geomagnetic pulsation and their propagation to low latitude ground stations are investigated. Numerical

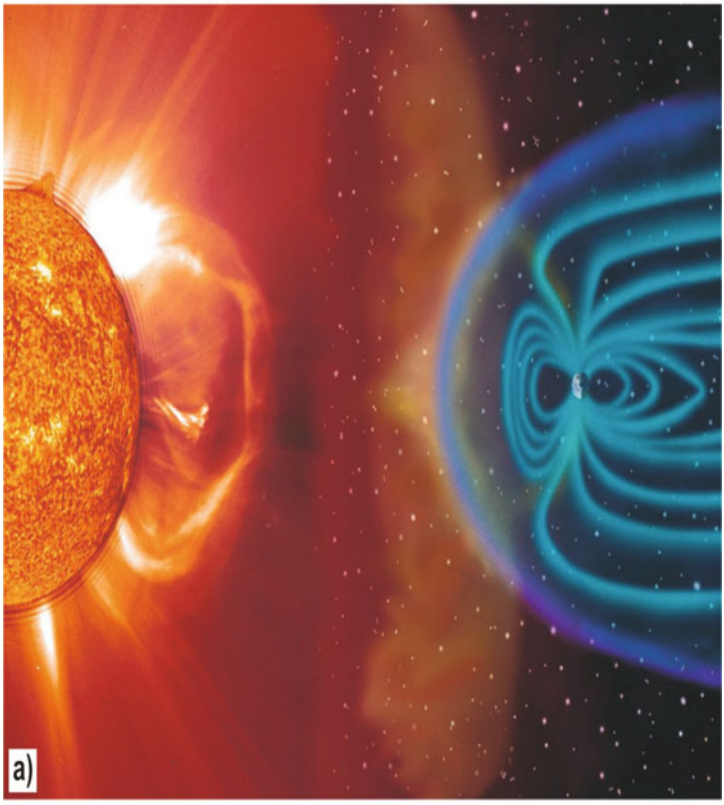

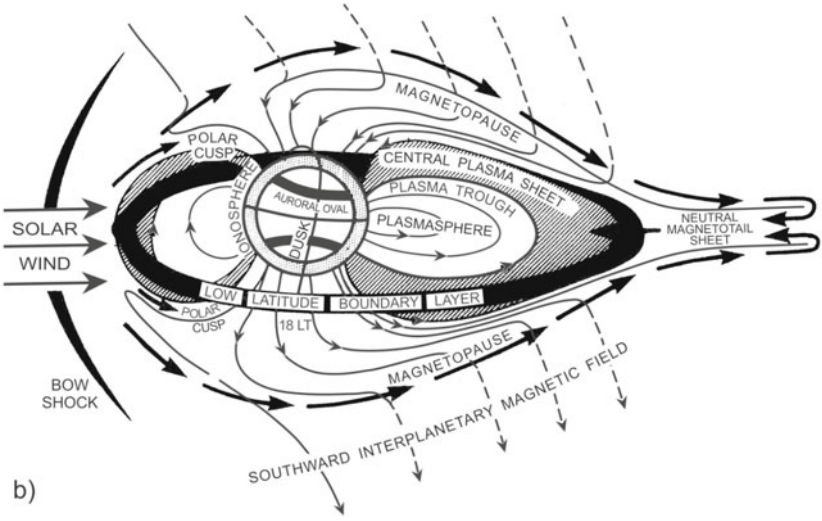

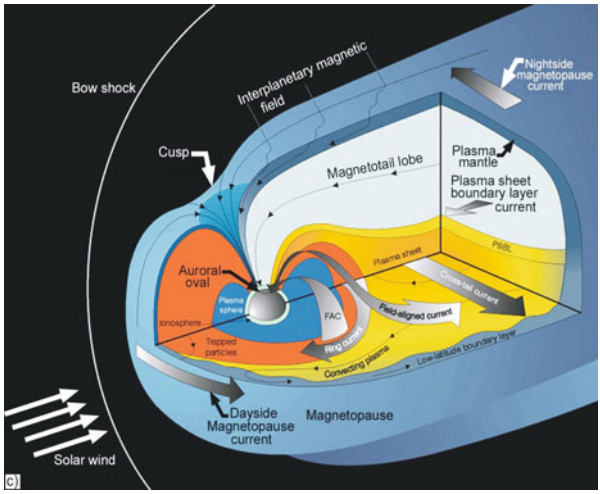

Figure 8.1. (a) Shelter from the storm. Clouds of hot gas called coronal mass ejections (CEMs) are often ejected by the Sun, when there is a large solar flare. It takes ~3 days for them to reach the distance of Earth's orbit. If they collide with Earth, the impact compresses and buffets Earth's protective magnetic field and can produce spectacular aurorae (Jardine, 2010). (b) Schematic polar cross sectional view of the Earth's magnetosphere, with its bow shock and the outflow of solar wind and interplanetary magnetic field from the Sun (Rajaram and Pisharoty, 1998). (c) An overview of different magnetospheric currents, which are setup in different regions by the charged particles flow (http://image.gsfc.nasa.gov/ presentation/cua_talk/sld004.html).

simulation codes are developed to study reconnection in 2D and 3D configurations. Magnetic topologies containing magnetic nulls are most susceptible to instabilities leading to reconnection.

I. International Magnetospheric Study

Upper atmospheric studies are not just restricted to the ionosphere, but extend to far-off space as well. Two essential ingredients for the formation of the magnetosphere are the EMF and the solar wind. The continuous flow of solar plasma is blocked by the EMF, confining it to magnetosphere. This process is vital to the existence of life on this planet. At the same time, this magnetic cavity filled up by tenuous plasma offers an excellent natural laboratory, helping throw up exciting new details by the world scientific community. Much is learnt about the dynamic plasma region over the past 40 years from the direct measurements by various spacecrafts (Chapter 3).

The solar wind carries the solar magnetic field out into space. Due to its extremely large electrical conductivity, solar wind plasma and solar magnetic field are tightly coupled, which means that the magnetic field is frozen into the plasma flow. At Earth orbit, the mean magnetic field strength is of the order of

7 nT. As the Earth rotates underneath the magnetosphere, a ground based observer sees different parts of the magnetosphere. Since the magnetosphere varies in time and space, the separation of temporal and spatial effects is not possible from a single location. Time variations are considerable and the magnetosphere never reaches a complete equilibrium because of continual flowing by solar wind. All models represent at best an interpretation of the time-averaged quiet magnetosphere. Measurements on the magnetosphere at different locations both in space and on surface are undertaken so that spatial and temporal effects are resolved and optimum use made of data.

More useful information about the temporal variability of solar magnetic activity is gained by the use of proxy data. Magnetic fields in the solar wind modulate the cosmic ray flux entering the Earth's atmosphere. These high-energy particles lead to the production of radioisotopes including ^{10}Be and ^{14}C, and so the abundance of these isotopes becomes a measure of solar magnetic activity; the abundance is anticorrelated with solar activity. The isotope ^{10}Be is preserved in polar ice-cores and its production rate together with the sunspot number is shown in Fig. 8.2. The figure clearly shows presence of the Maunder minimum and that, although sunspot activity is largely shut off during this period, cyclic magnetic activity continued with a period of ~9 years. The ^{10}Be record extends back over 50 ka and analysis of this record clearly shows

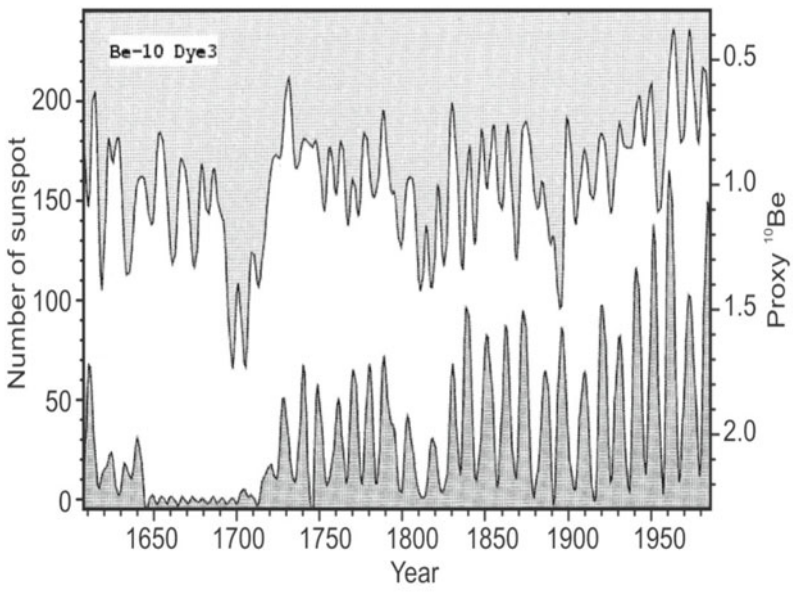

Figure 8.2. Comparison of the proxy ^{10}Be data from the Dye3 ice core (measured in 10^3 atoms/g) filtered using a low pass (6 year) filter, with the filtered (6 year) sunspot group number as determined by Hoyt and Schatten (1998). Note that the ^{10}Be is anticorrelated with sunspot activity (Tobias, 2007).

continued presence of the 11-year solar cycle. Analysis also indicates that the Maunder minimum is not an isolated event, but a regularly spaced minima (termed grand minima) interrupting the record of activity with a significant recurrent timescale of 205 years. The variations in ^{14}C production confirm this pattern of recurrent grand minima with a time scale of ~200 years. Moreover, both of these radioisotope records show significant power at a frequency that corresponds to roughly 2100 years. It appears as though grand minima occur in bursts.

Particles, substorms, whistlers: The basic understanding of the magnetosphere, combined with availability of high quality detectors for charged particles, waves and fields, on rockets and satellites of high reliability and with good telemetry, makes it timely to study numerous phenomena quantitatively.

One major area of study is the transfer of charged particles and energy from the solar wind into the magnetosphere. The major mechanism of energy transfer from solar wind to the Earth's magnetosphere is magnetic reconnection (Fig. 8.3). If the interplanetary magnetic fields (IMFs) are directed opposite to the EMFs, there is magnetic erosion on the dayside magnetosphere (by magnetic connection) and magnetic field accumulation on the nightside magnetotail region. Subsequent reconnection on the nightside leads to plasma injection at these local times and auroras occurring at high latitude nightside regions. As the magnetotail plasma gets injected into the nightside magnetosphere, the energetic protons drift to the west and electrons to the east, forming a ring of current around the Earth. The ring current causes a diamagnetic decrease in the EMF measured at near-equatorial magnetic stations. The decrease in the equatorial magnetic field strength is directly related to the total energy of the ring current particles and thus a good measure of the energetic of the magnetic storm.

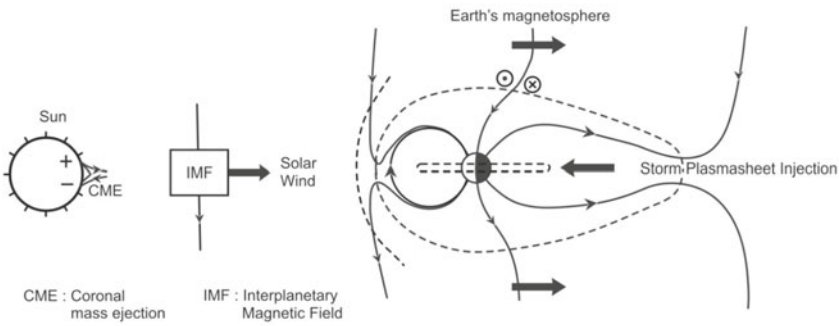

Figure 8.3. A schematic showing the magnetic reconnection process.

The storage of particles in the reservoirs of the plasmasphere and the plasma sheet and dynamics of these regions is another area of study. Propagation of very low frequency (VLF) whistlers enables the plasmapause to be identified and its movement followed. The substorm is an important natural perturbation of the magnetosphere. Magnetic energy accumulated in the tail is suddenly released and dumped in the auroral regions by charged particles. Substorms can either occur in rapid succession at the rate of several an hour as part of a magnetic storm (usually caused by solar flare induced effect) or separated by several days. It seems that a substorm may be triggered by the IMF turning southwards. During growth phase, the dayside boundaries are moved inwards towards the Earth and thus project to lower latitudes (Chapters 3 and 5).

Wave particle interactions are also of importance in the magnetosphere. The threshold electron energy for cyclotron resonance as a function of radial distance in the equatorial plane is shown in Fig. 8.4. In the cyclotron resonance, low energy waves propagating in the whistler mode resonate with trapped electrons of the appropriate cyclotron frequency; the wave amplitude can increase and the particles suffer pitch angle scattering so as to align their motion more along the field and so down to the atmosphere where they are lost by collision. While this theory of wave-particle interactions is incomplete, it does demonstrate that very high energy particles may be unstable everywhere and

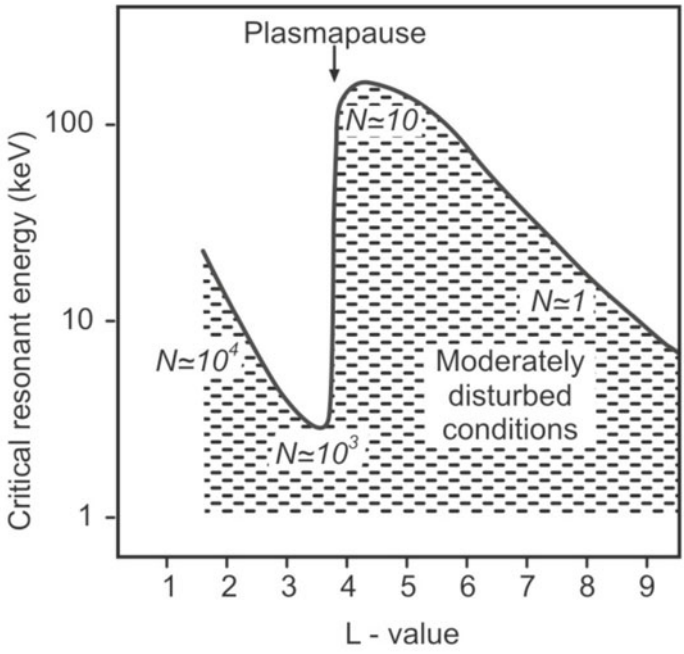

Figure 8.4. Threshold energy for unstable cyclotron resonance plotted against radial distance in the equatorial plane in Earth radii (L). N is the plasma density in particles/ cm^3 (Woolliscroft, 1978).

that electrons with over 10 keV are stable in the radiation belt. The transfer of magnetospheric energy down to the ionosphere and the atmosphere with possible effects on the weather is also studied.

Satellite use: Central to the success of the international magnetic study (IMS) are about a dozen dedicated satellites, of which the most important is the European space agency's GEOS satellite. GEOS is making valuable measurements on the magnetospheric plasma and waves. In particle terms the significance of electrostatic waves is now apparent. Complimentary to GEOS is the ISEE (international Sun-Earth explorer) spacecraft, apart from a number of other satellites such as Hawkeye and S3-2 and 3, which are making relevant measurements. Surface magnetic field measurements are also a valuable tool to study the magnetosphere. Continuous monitoring of the magnetosphere with magnetometers, unlike optical measurements, does not depend on the weather and is relatively cheap and reliable. The magnetospheric current systems, thus can be determined unambiguously with existing networks of high resolution magnetometers in addition to the ~200 magnetic observatories. In a similar manner, ground-based networks of ionosondes, riometers, low-frequency radio wave receivers and optical instruments aid magnetospheric study.

Two equatorial flights in April and Sept 1998 launched from the Indian low-latitude station SHAR detected plasma bubbles restricted to a narrow longitudinal extent. Plasma parameters are measured under two different conditions in the post-sunset ionosphere, when the F layer is moving upward (19:21 IST launch) and when the F layer is stationary (20:41 IST launch). Low altitude bubbles during upwelling of the F region in pre-reversal current enhancement phase are characterized by turbulent non-Maxwellian regions. Transitional scale waves with $k = 3.6$ are observed in the bubbles. This flight also detected strong sharp E layers during down leg and an intermediate layer at 170 km. Night-time bubbles during almost stationary F layer conditions show turbulent Maxwellian features with moderate cooling compared to the undisturbed environment. Transitional scale in the bubble region shows a spectral index $k = 3.1$. The spectral power is reduced by ~20 dB compared to the sunset flight.

II. Boundary Layer Waves and Auroras

Plasmas are generally far from their thermodynamic equilibrium states, and hence contain some amount of free energy, which can generate several kinds of plasma modes in the magnetospheric boundary layers such as magnetopause boundary layer, plasma sheet boundary layer, polar cap boundary layer (PCBL) and others (Fig. 8.5).

Polar observations indicate the presence of intense broadband plasma waves nearly all of the time (with ~96% occurrence frequency) near the apogee of the

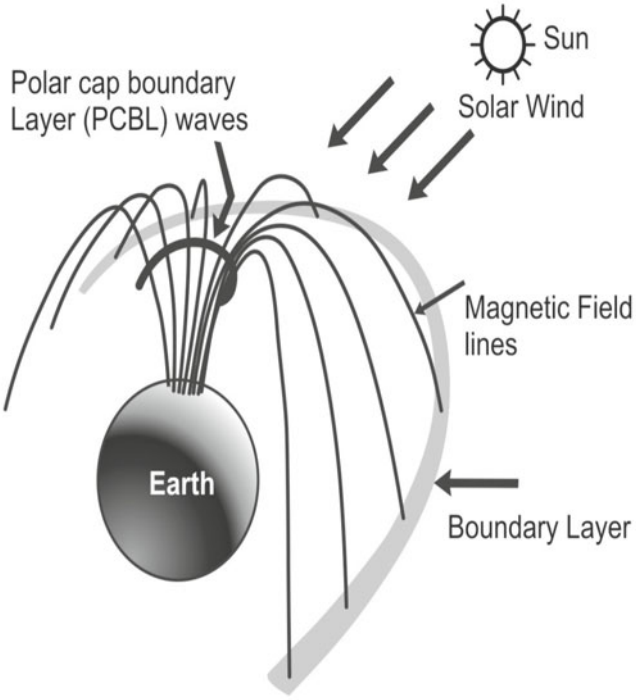

Figure 8.5. A northern polar view of the mapping of polar cap boundary layer waves to the low-latitude boundary layer (Tsurutani et al., 2003).

polar trajectory (~6-8 R_E). The region of wave activity bounds the dayside (0500-1800 LT) polar cap magnetic fields, and thus these waves are called PCBL waves. The waves are spiky signals spanning a broad frequency range from a few Hz to more than 20 kHz having a rough power law spectral shape. The wave magnetic component appears to have an upper frequency cutoff of the electron cyclotron frequency. The electric component extends well beyond the electron cyclotron frequency. The waves are possibly a mixture of obliquely propagating electromagnetic whistler mode waves and electrostatic waves. There are no clear intensity peaks in either the magnetic or electric spectra, which can identify the plasma instability responsible for generation of PCBL waves.

The wave character (spiky nature, frequency dependence and admixture of electromagnetic and electrostatic components) and intensity are quite similar to those of low-latitude boundary layer (LLBL) waves detected at and inside the low-latitude dayside magnetopause. Because of the location of PCBL waves just inside the polar cap magnetic field lines, it is natural to assume that these waves occur on the same magnetic field lines as the LLBL waves, but at lower altitudes, where the most likely scenario is that field-aligned currents

or current gradients locally generate the waves. A strong relationship is found between the presence of ionospheric and magnetosheath ions and the waves near the noon sector. These waves may thus be responsible for ion heating observed near the cusp region. Anti-sunward convection of these freshly accelerated O^+ ions over the polar cap during intense wave events (occurring during southward B_z events) might lead to enhanced plasma sheet O^+ population. For magnetic storm intervals, this mechanism leads to a natural delay between the main phase onset and the appearance of oxygen ions in the ring current.

High time resolution waveform observations by plasma wave instrument onboard the Geotail, Polar and FAST spacecrafts have shown broadband high frequency plasma waves consisting of a series of bipolar solitary pulses. Various models based on solitons/double layers and phase space holes are developed to explain the characteristics of these solitary structures.

III. Ionosphere-magnetosphere Coupling Studies

One of the outstanding questions of magnetospheric physics is associated with ionosphere-magnetosphere coupling. Ionosphere and magnetosphere are closely linked together via magnetic field lines, e.g. cold ionospheric electrons and ions (e.g. O^+) drift into the Earth's magnetospheric regions, namely plasmasphere, plasma sheet and tail lobes. The change in magnetospheric ion composition (especially increased O^+ ions) can have large effects on some important magnetospheric processes. The two missions, active magnetospheric particle tracer explorers (AMPTE) and the combined release and radiation effects satellite (CRRES) showed ionized oxygen escaping from the upper atmosphere could play a critical role in electromagnetic processes in the near-Earth space.

Several plasma instabilities are studied in presence of O^+ ions in the Earth's plasma sheet and ring current region. A theoretical model is developed to study Kelvin-Helmholtz modes driven by O^+ in the Earth's plasma sheet region (Fig. 8.6). The role of these modes is investigated in magnetosphere-ionosphere coupling processes, namely magnetic storm and substorm, and low-frequency turbulence. It is found that the presence of ionospheric-origin O^+ ion beams with anisotropic pressure can excite helicon mode instability in near-Earth plasma sheet region, provided their Alfvenic Mach numbers lie in certain range. The helicon modes are easily excited under the conditions when the usual long wavelengths fire-hose modes are stable. It is shown that the anisotropic O^+ ions in the ring current can excite low-frequency quasi-electrostatic waves (Fig. 8.7). The scattering of ring current particles by these low-frequency electrostatic waves could lead to ring current decay and thus provides a mechanism that is complimentary to charge exchange.

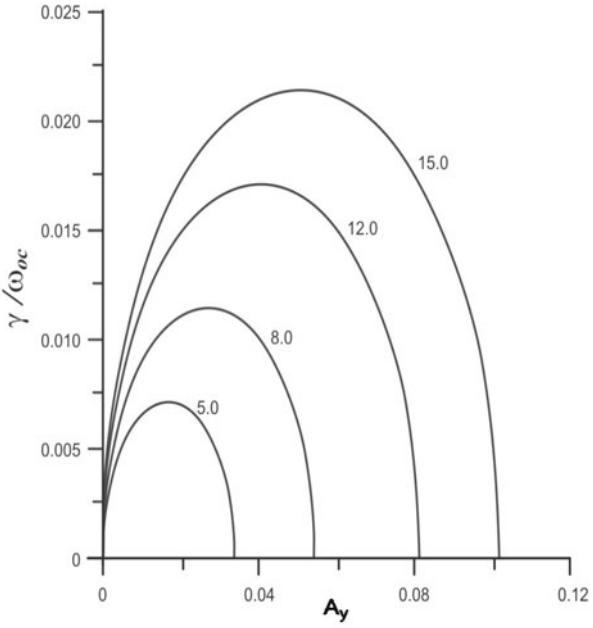

Figure 8.6. Variation of normalized growth rate γ/ω_{oc} with normalized parallel wave number A_y for the shear flow instability driven by O^+ ions in the plasma sheet region, for the parameters; normalized wave number $A_y = 600$, ratio of proton to oxygen density e = 2.0 and normalized shear S = 5, 8, 12, 15, $A_y = 600$, e = 2.0 (Kakad et al., 2003).

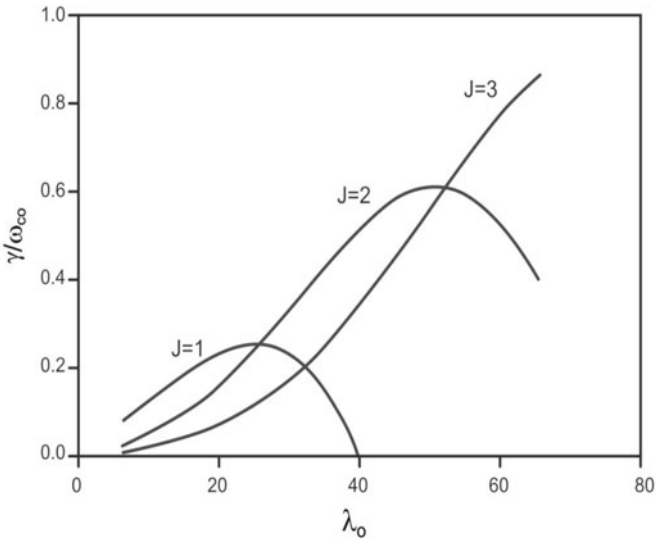

Figure 8.7. Comparison of growth rates for anisotropic index J for low frequency waves (Singh et al., 2004).

IV. Numerical Modelling

Global studies have opened innumerable observations that need to be established on theoretical platform. This can only be done through numerical modelling by incorporating various complex parameters in the code explaining observations in terms of associated physics related to transport of energy, momentum and mass transfer between the solar wind and magnetosphere. Plasma instabilities during sub-storm, which give rise to anomalous resistivity leading to generation of parallel electric fields, are being numerically modelled. The magnetosphere-ionosphere coupling during magnetospheric storms and substorms as well as the generation mechanisms of magnetic pulsations and their propagation to low latitudes is under close scrutiny (Fig. 8.8). Efforts are also directed towards developing magnetohydrodynamic simulation codes for investigating magnetotail dynamics that result in large scale electric fields in the magnetosphere.

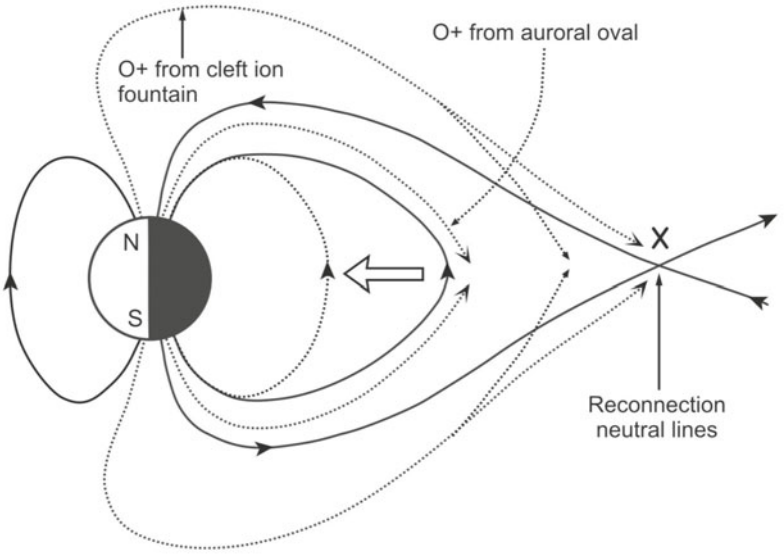

Figure 8.8. A schematic illustration of the respective paths into the magnetosphere of oxygen ions from the dayside cleft and the nightside auroral ionosphere (Gazey et al., 1996).

8.1 SPACE WEATHER EFFECTS

Modern society relies on technology, which is affected by conditions in space environment. Space weather refers to conditions between the Sun and Earth encompassing the solar wind, interplanetary space, magnetosphere, ionosphere and thermosphere. These conditions can influence the performance and reliability of space-borne and ground-based technological systems and can endanger human life or health.

Space weather disturbances caused by enhanced stream of solar plasma during solar flares and CMEs are known to disrupt communications, endanger satellite payloads and introduce severe errors in a variety of tracking and positioning systems (Fig. 8.12). The phenomena of geomagnetic storms are the most obvious features of space weather disturbances. Consequently, the geomagnetic response to differing solar conditions also varies to a wide extent. Some of these effects noticed during the intense magnetic storms are described in Figs 8.9–8.11.

I. Proton Flux Characteristics and Space Weather

Solar flares are the manifestations of the tremendous eruptions in the solar atmosphere, producing sudden energy release. The magnitude of magnetic energy thrown out in the solar chromospheres and corona during intense flares range between 10^{28} and 10^{34} ergs, energizing electrons and ions up to MeV and GeV respectively. During the high solar activity periods, active regions produce large fluxes of energetic flare particles to CME related shocks, which accelerate the solar energetic particle (SEP) events. Mass ejections play a dominant role in driving large geomagnetic storms by causing sudden commencements on the magnetic records produced by transient interplanetary shocks. Geoeffective nature of the solar disturbances and the energy transfer mechanism of the solar wind energy into the magnetosphere through the reconnection of IMF, are seen to take place.

A major solar flare eruption (Fig. 8.9) occurred at 1620 UT on 4 Nov 2001 followed by strong solar radiation storm and proton event. This was recorded

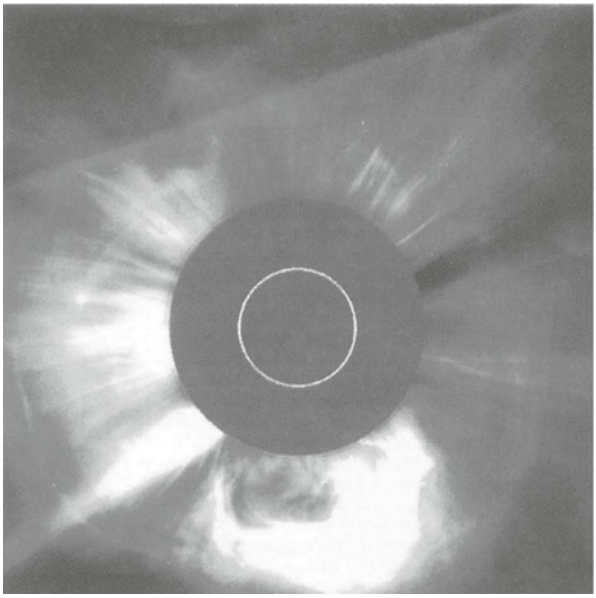

Figure 8.9. Coronal mass ejection or solar flare (http://www.nasa.gov/vision/universe/watchtheskies /july7_cme.html).

by SOHO and other interplanetary satellites. CME associated with the flare event triggered an interplanetary shock, which affected the geomagnetic field after ~33 hrs. The shock impact was quite intense to produce SSC magnitude of ~100 nT in H in low latitude ground magnetic records followed by sharp and deep main phase ($D_{ST} < -250$ nT) in the first stage, following the density (N_P) enhancement. High time resolution digital data from the equatorial and low latitude stations in India analyzed the influence of various interplanetary

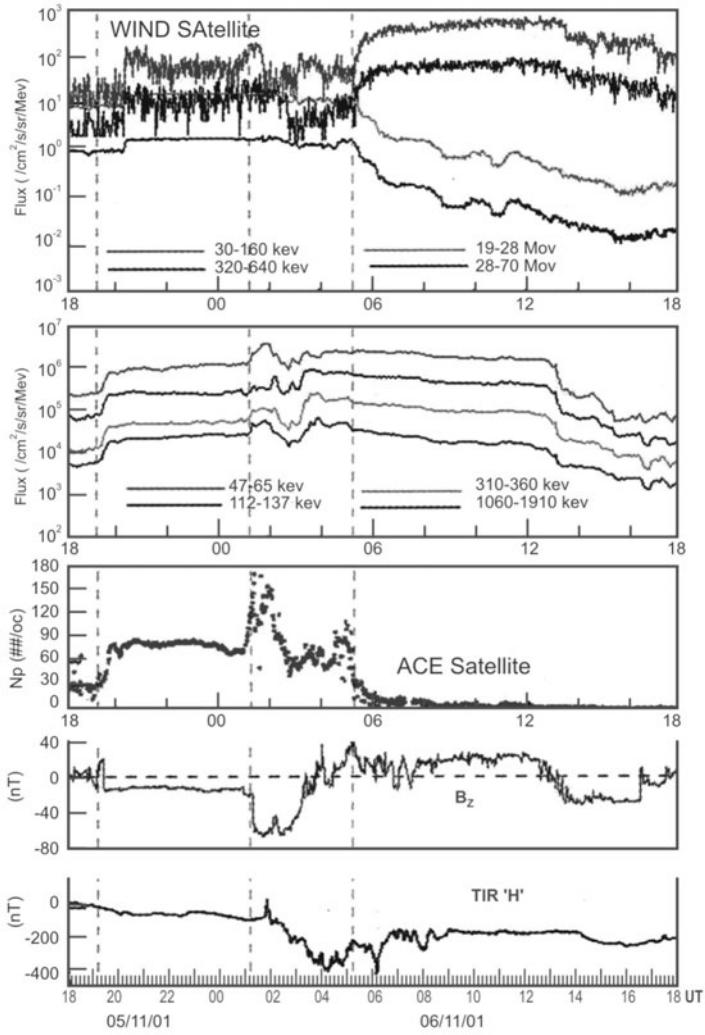

Figure 8.10. Proton flux intensities, as recorded by the ACE and WIND spacecraft, proton density N_P, IMF component B_z (ACE) and the variation in the H component at Tirunelveli (TIR) during 5-6 November 2001. Three dashed vertical lines shown represent the time corresponding to intense proton density enhancements (Alex et al., 2005).

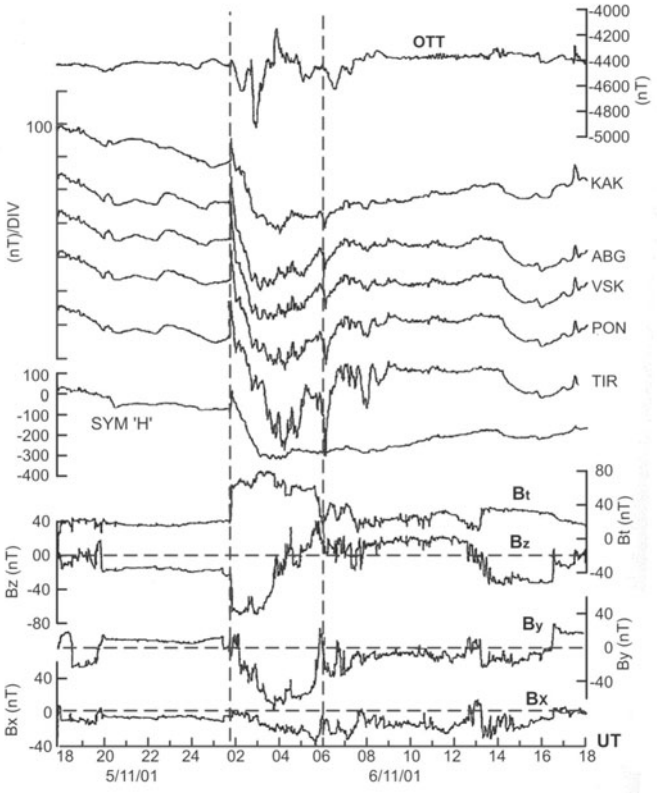

Figure 8.11. Shock effect in the equatorial, low and mid latitude digital magnetic records, seen as the sudden commencement (~80 nT) at 01:50 UT on 6 November 2001. Formation of intense main phase corresponding to the large B_Z of magnitude -70 nT is the salient feature of the event. Satellite data in time is shifted by 35 min. The first vertical line corresponds to the SSC onset and the second one indicates the peak time of development of substorm (Alex et al., 2005).

parameters on the intensity and duration of the magnetic storm. A double step storm was found to be in progress caused by multiple injections. During the period of recovery, after a lapse of 8 hrs, a third stage of depression in ground magnetic field was set in, which corresponded to the southward directed B_Z.

In order to understand the emission features of the particle energy accompanying the solar energetic proton event of 4 Nov 2001, proton flux of various energy levels from the ACE and WIND are given in the topmost panel of Fig. 8.10. Vertical dashed lines are marked against the recurring trend of enhancements in the particle flux densities during 5-6 Nov 2001. Following the strong X-ray flare at 16:20 UT on 4 Nov, proton flux showed sharp increase at all the energy levels as observed by WIND and ACE satellites (Fig. 8.10). The N_P as recorded by ACE satellite is considerably low on 4 Nov and a gradual increase is seen in the early hours of 5 Nov. Around 19 UT, a sudden jump in density is quite evident coinciding with second in N_P flux.

Figure 8.11 brings out the shock effect and magnetic storm characteristics as recorded from the interplanetary parameters by ACE and ground digital magnetic data records from the equatorial, low and mid latitude locations for 5-6 Nov 2001. The arrival of shock is conspicuous at all the locations from the SSC magnitude of ~80 nT, in the equatorial, low and mid latitude digital records. The ring current intensity parameter 'symH' (WDC, Kyoto) indicated that the symmetric component of ring current had a maximum magnitude of the main phase intensity ~–300 nT. The magnetic variation at mid latitude station Ottawa (OTT) given in the topmost curve, showed maximum negative deviation ~500 nT corresponding to the main phase period at the low latitudes. Second vertical dashed line shown at 06:20 UT of 6 Nov, marks the second minima during the recovery phase, which coincides well with the peaked positive value of ~20 nT in B_Y with a lag of ~20 min.

II. Geomagnetic Storm Effects on Technology

The following are the space weather effects on the technological systems:

(i) Solar eruptions directed towards the Earth are potentially harmful to advanced technology. Advancement in technology has been immense in communication, navigation and space-borne satellite systems. Modern instruments and links around the globe are increasingly dependent on electricity and electronics. Technological systems in space and on the Earth's surface are subjected to adverse effects from geomagnetic disturbances. During such events, the magnetospheric compression by the solar wind forces the magnetospheric boundary inward past the geostationary satellite position (Fig. 8.12).

(ii) Geosynchronous communication satellites orbiting the Earth are many in number. A large geomagnetic storm enhances the electrons and ions hitting these satellites, leading to intense spacecraft charging that damages the spacecraft.

(iii) Enhanced levels of solar radiation associated with intense flare activity on the Sun also cause heating and expansion of neutral atmosphere and increase the amount of atmospheric drag that a satellite experiences in an unpredictable manner.

(iv) Auroral activity and intense substorm disturbances cause dropouts and changes in paths of HF communication and increased scintillation degradation of radio signals at high frequencies and disrupt surveillance tracking of the satellite.

(v) The disturbance also induces extra currents in the wires of electrical power grid, producing temporary overload. Such severe geomagnetic disturbances induce DC currents in power lines and can cause destruction of power station transformers.

(vi) Geomagnetically induced currents and voltages can also damage long pipelines and communication cables. These currents affect the conductors used for telecommunications.

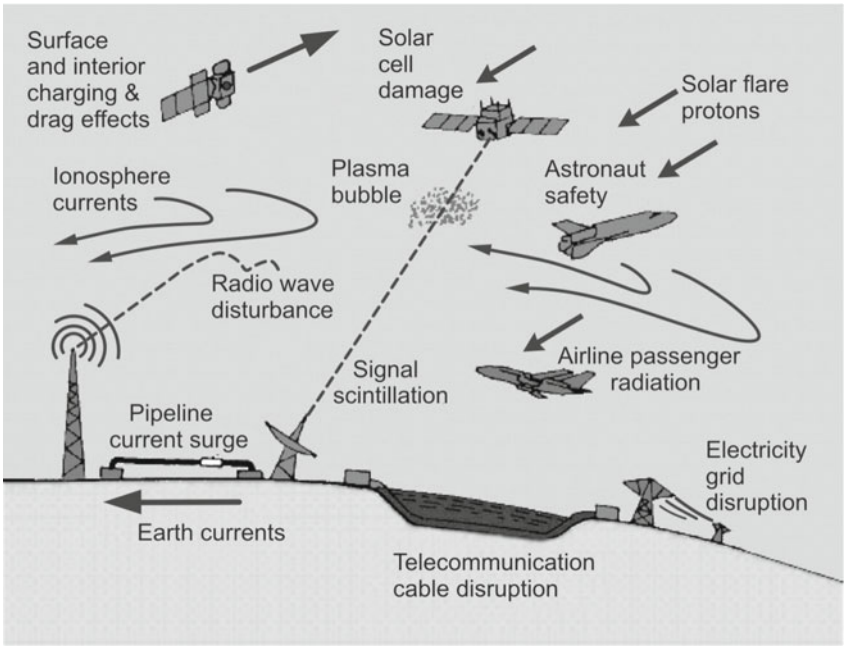

Figure 8.12. Space weather effects on the technological systems ranging from disruption in satellite communication to the destruction in power lines and underground cable (Lakhina and Alex, 2003).

(vii) Very high energy (~1 MeV) charged particle fluxes released during storms and substorms pose a serious retardation health hazard for astronauts. Chapter 9 provides details for items (i) to (vii).

III. Infrastructure for Space Weather Research in India

Several institutes and university departments are participating on various programmes associated with solar physics, interplanetary plasma and magnetic field, magnetospheric physics, ionospheric physics and atmospheric physics that form the backbone for space weather programme. Most of the scientists utilize solar, interplanetary and magnetospheric data from various NASA missions from 1970 onwards for modelling the medium and for the study of dynamics and instabilities in the regions. On the experimental side, expertise for HF Doppler radar, VHF, MST and partial reflection radars exists. Several ionosonde and airglow experiments provide data to understand the ionospheric irregularities. Excellent facilities for monitoring the Sun exist at solar observatories in Udaipur, Ooty and Kodaikanal. A brief summary of the existing infrastructure in India for space weather-related research activities is given in Table 8.1.

Table 8.1 Infrastructure available for space weather-related activities

Organizations/Universities	*Experiments*	*Investigations/activities*
Andhra University, Waltair	Airglow photometer; Digital ionosonde; HF Doppler radar	Ionosphere-thermosphere study; E- and F-region dynamics
Banaras Hindu University	Fabry-Perot spectro-photometer; Dual frequency microwave radiometer; ELF, VLF experiments by Whistler observations	For measuring thermospheric temperature and winds, air pollution; Whistler studies; Ionosphere magnetosphere dynamics
Baraktulla University, Bhopal	Radio beacon studies; Whistler measurements	Plasma irregularities; Ground-based technique for probing the inner magnetosphere
Bhabha Atomic Research Centre, NRL, Trombay	Cerenkov telescope at Mt.Abu	Study of gamma ray sources and the cosmic ray mass composition
Indian Institute of Astrophysics, Bangalore	Digital magnetometer; Digital Ionosonde	Ionosphere-thermosphere coupling; Solar-terrestrial relationships
Indian Institute of Geomagnetism, Mumbai	Network of 11 magnetic observatories; Digital fluxgate magnetometer set-up at six observatories; MF (1.98 MHz) radars at Tiruneveli and Kolhapur; Radio beacon experiments; Scanning photometer; Tilting photometer; All sky imaging camera at Kolhapur; TEC deduced from GPS measurements; CRABEX Experiment	Solar-Terrestrial physics; Magnetic storms and substorms; Secular variations; Geomagnetic activity; Forecasting and space weather; Theoretical and simulation studies on storm-substorms phenomena; Mesosphere winds, tides and planetary waves; Plasma irregularities; Monitoring nightglow emissions at different wavelengths; Atmospheric gravity waves and F-region irregularities; Ionosphere-thermosphere dynamics and Ionospheric tomography
ISRO Satellite Centre, Bangalore	Scanning sky monitor (SSM) for Indian Astronomy satellite; Solar X-ray spectrometer for GSLV: CRABEX	To study the long-term variability in bright X-ray sources for studies of variable stars; To study X-ray flux from Sun over 2 keV to 10 MeV energy range; Ionospheric tomography
Kerala University	HF Doppler radar data	To study the ionospheric plasma drift
National Geophysical Research Institute	Magnetometers at two locations	Studies related to low latitude magnetic variations

National MST Radar Facility (NMRF), Tirupati	MST (53 MHz) radar at Gadanki; Rayleigh lidar system	Studies of long period atmospheric waves, ionospheric irregularities; Temperature profiles at 5-85 km altitude range
National Physical Laboratory, New Delhi	Digital ionosonde; GPS, Radio beacon studies; RPA experiment on SROSS-C2; SASCOM Data Centre Lidar: Laser heterodyne system	Ionospheric plasma parameters and plasma irregularities; Total electron contents; Dissemination of data for global change related studies; Measurements of ozone, water vapour. etc.
Osmania University, Hyderabad	Ionospheric scintillation experiment	Ionospheric irregularities
Physical Research Laboratory, Ahmedabad	High resolution IR Fabry-Perot spectrometer; Ionosonde; All sky imaging camera; Fabry-Perot spectrometer at Mt. Abu; Coherent radio beacon experiment; Nd:YAG backscatter lidar at Mt. Abu	Observations of bright diffuse nebulae associated with star forming regions; Ionospheric plasma properties and ionospheric irregularities; Measurement of neutral thermospheric temperature and wind; Total electron content (TEC), ionospheric tomography; Vertical structure of atmospheric density and temperature around 90 km
Survey of India, Dehradun	One permanent magnetic observatory at Sabhawala	For studying the low latitude current system, Secular variation pattern
Tata Institute of Fundamental Research (TIFR), Mumbai	Ooty radio telescope; GMRT	Observations of high resolution interplanetary scintillations; Probing of inner heliosphere from 0.2-0.8 AU by IPS
Udaipur Solar Observatory of PRL, Ahmedabad	GONG telescope; Sun photometer; Solar X-ray spectrometer; Full disk telescope	To probe interior of the Sun using helioseismology; To study solar eruption processes, the solar flares, CMEs, etc.; Observations of soft X-rays from the Sun; Hα synoptic observation of solar activity
University of Rajkot, Gujarat	ELF, VLF measurements; Radio beacon experiments	Electromagnetic wave propagation in the ionosphere and magnetosphere; Ionospheric irregularities
Vikram Sarabhai Space Centre, Trivandrum	HF and VHF Doppler radar; Digital ionosonde; Langmuir probe measurements; Rayleigh lidar	Measurements of Doppler velocities and spectral width to study the ionospheric irregularities; Ionospheric E- and F-region parameters; E-region plasma properties; Vertical structure of atmospheric density and temperature from 5 to 85 km

8.2 IONOSPHERIC ELECTRODYNAMICS: SHORT PERIOD FLUCTUATIONS

The ionosphere has day-to-day weather that affects technologies in navigation and communication. A space weather modelling capability is useful for mitigating technology impacts. Observations of the ionosphere are sparse. The sparseness does not allow for a full ionospheric specification from data only. Empirical models are based on rough averaging of these sparse data. But the dynamic character of the ionosphere causes large differences between the empirical model result and observations. Ground-based observations on ionospheric scintillations, geomagnetic pulsations, partial radar and airglow experiments are discussed below.

The solar radiation is capable of splitting the neutral atmospheric constituents into ions and electrons leaving the atmosphere in an ionized state. The ionization affects short wave radio communication. The free electrons in the ionosphere are not uniformly distributed but form layers (Chapter 3). Furthermore, clouds of electrons (known as travelling disturbances) may travel through the ionosphere and give rise to fluctuations in the signal. The effects include scintillation, frequency change, and micropulsations. All these effects decrease as frequency increases. This ionized air moving across the EMF favours a dynamo to generate daytime electric currents. Typical altitude profiles of the mid-latitude electron density at day and night for years of minimum and maximum solar activity are shown in Fig. 8.13.

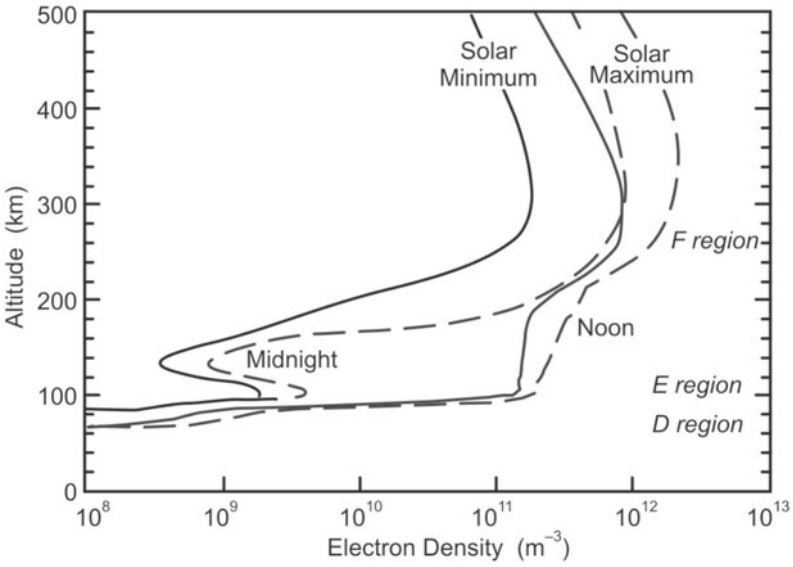

Figure 8.13. Altitude profiles of electron density at 18°N, 67°W, September equinox, representative of noon and midnight, solar minimum (solid lines) and solar maximum (dashed lines), with F, E and D regions indicated (Richmond, 2007).

The ionosphere refracts, reflects, retards, scatters and absorbs radio waves depending on wave frequency. Around the Earth, communications are possible by utilizing ionospheric and ground reflections of waves at frequencies below ~3–30 MHz (10 to 100 m wavelength), depending on the peak electron density. However, frequent collisions between electrons and air molecules in the D region remove energy from radio waves, leading to partial or complete absorption. At higher frequencies, radio waves penetrate entirely through the ionosphere allowing radio astronomy and communications with spacecraft. Nevertheless, such signals can still be degraded by refraction and scattering off small scale density irregularities. In case of GPS geolocation signals, variable ranging errors are introduced by ionospheric signal retardation. The retardation is proportional to the total electron content (TEC) or height-integrated electron density. A typical global pattern of TEC is shown in Fig. 8.14, which shows TEC larger in winter than in summer, because of slower chemical loss in winter.

Radio waves of frequencies in the very high frequencies (VHF) or higher ranges transmitted from satellites and received on the Earth, often encounter ionospheric irregularities in their path. The intensity pattern produced on the ground as a result of scattering of radio waves by the irregularities, results in temporal variations or scintillations in intensity of the signal recorded by the receiver. The phase of the wave also undergoes scintillations. Study of ionospheric scintillations provides a relatively inexpensive tool for monitoring the development of equatorial ionospheric irregularities in the equatorial spread F (ESF), which has its origin in plasma instabilities. There is a great deal of

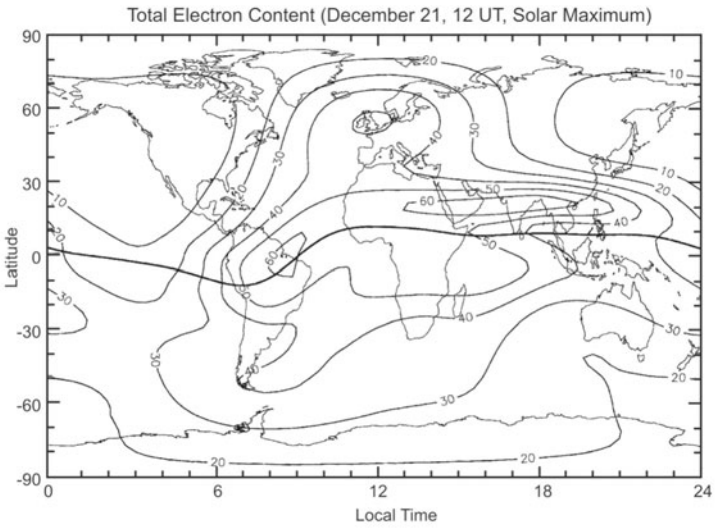

Figure 8.14. Global map of TEC at 12 UT, December solstice, solar maximum. Local time increases with longitude as shown on the bottom scale. Contours are spaced at intervals of 10×10^{16} electrons/m^2. The thick solid line is the magnetic equator (Richmond, 2007).

interest in the prediction of ESF which affects satellite communications and cause loss of phase lock for GPS satellites, particularly in a period around sunspot maximum (Chapter 9).

I. Ionospheric Irregularities and Radio Wave Scintillation

Ionospheric scintillations are variations in the amplitude, phase, polarization, or angle of arrival of radio waves. They are caused by irregularities in the ionosphere, which change with time. The main effect of scintillation is fading of signal. The fades can be quite severe, and they may last up to several minutes. They impose hazards on communication system through degradation in analog and bit rate errors in digital communications. The equatorial region comprising ±20° about the magnetic equator is particularly prone to scintillation activity after sunset. The basic purpose of scintillation studies is to extract irregularity parameters like amplitude of the density deviation, scale size and its distribution, drift, anisotropy and spatial distribution of the irregularities. This knowledge is used in developing models to minimize the problems due to fading of signals, and provide sufficient signal margins.

A chain of VHF polarimeters and scintillation recorders are used to study generation and movement of the ionospheric plasma irregularities, which cause radio scintillation. The radio source used for these studies is the 244 MHz signal from the ETS-2 satellite at 136°E for measurement of total ionospheric electron content. Three-channel PC based data logger capable of sampling data at 10 Hz is used in acquiring scintillation data. Typical scintillation records are shown in Fig. 8.15.

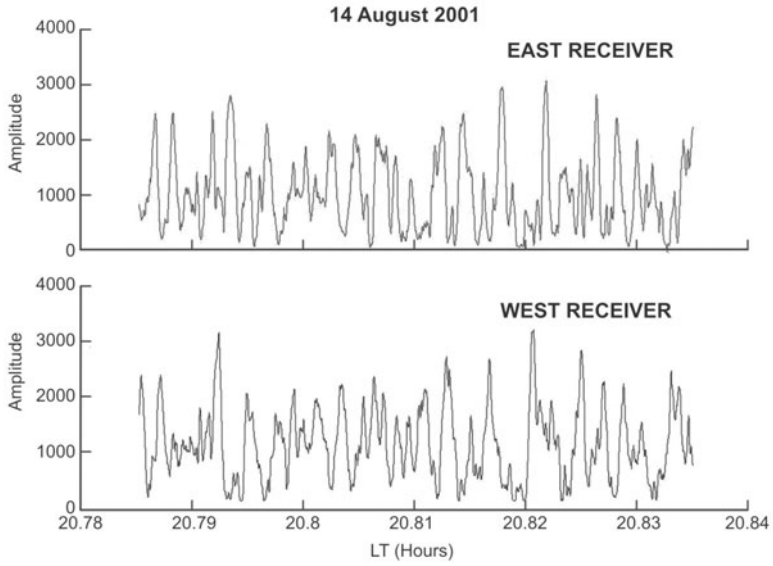

Figure 8.15. Scintillation records collected at Tirunelveli on 14 August 2001.

Daytime scintillation associated with E region irregularities are generally weaker than nighttime scintillations due to F region irregularities (range or frequency spread-F). Nighttime scintillations are continuous near the dip equator, but discrete patches of varying durations are seen at stations far off from it. Figure 8.16 shows the onset of scintillation recorded at Tirunelveli, Pondicherry and Mumbai on the night of 2 Dec 1995. A delay in onset time is seen when one moves away from equator. Equatorial scintillations are inhibited with increase in magnetic activity and this effect also shows seasonal and solar activity.

Figure 8.17 shows effect of sunspot activity on the morphology of the occurrence of scintillation. With an increase in sunspot number, mean percentage occurrence of scintillations increases at both equatorial station and at temperate station Mumbai. During low solar activity period from 1993 to 1996, percentage occurrence is higher at Ujjain than at Mumbai due to mid-latitude generation. Low-latitude scintillations can be either inhibited or triggered during storms depending on the phase of storm and its local time of occurrence.

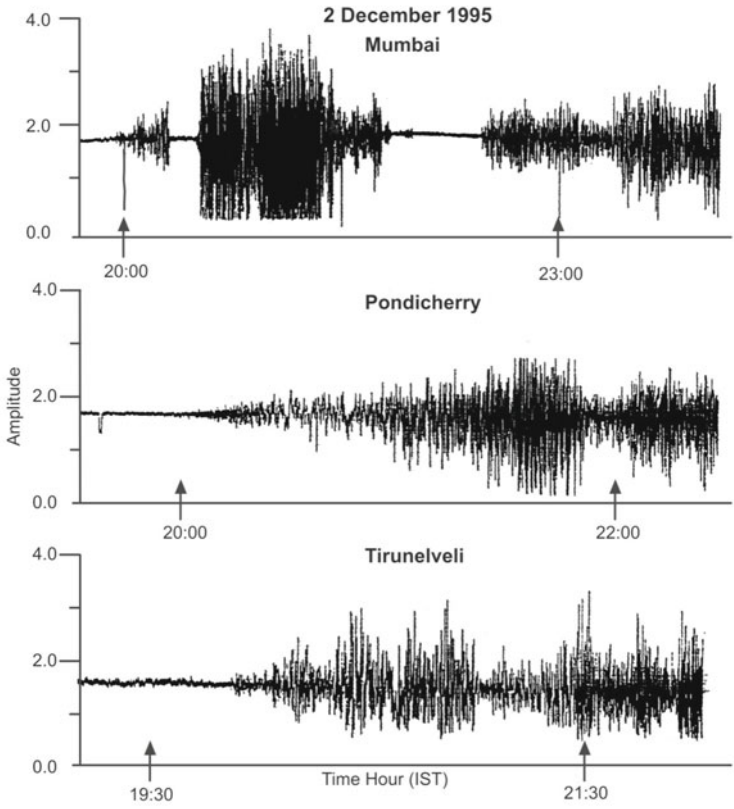

Figure 8.16. Example of scintillation onset on 2 December 1995 for three stations situated at different latitudes (Banola et al., 2005).

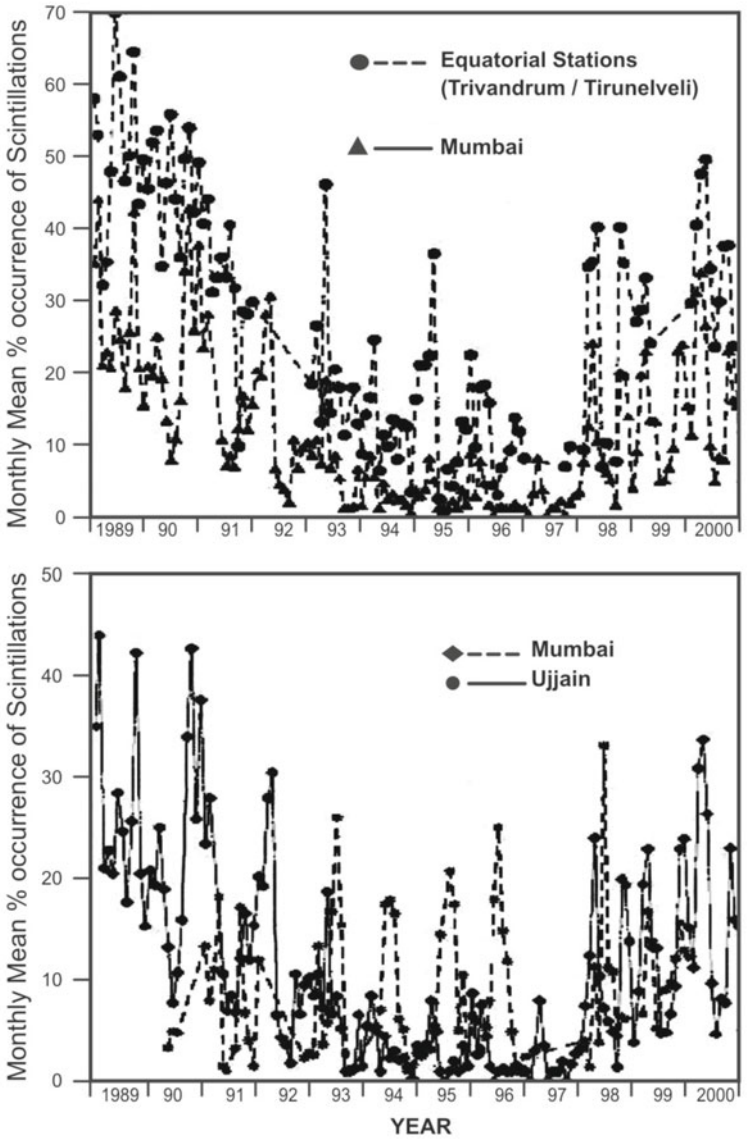

Figure 8.17. Effect of solar activity on the occurrence of scintillations at equatorial stations, Mumbai and Ujjain.

Fresnel frequencies deduced from the power spectra show transverse drift velocities of irregularities to vary between 40 and 118 m/sec, while decorrelation distance varied from 68 m to 188 m for the Indian region. Spectral indices vary in the range from 2.9 to 6.21 with a mean spectral index of 3.4 corresponding to scale sizes of 20–1000 m.

Boundary of equatorial scintillation is defined as dip latitudes, at which the occurrence of scintillation is reduced to half of its value at the magnetic

equator. This is estimated for solar cycle 1989–2000 using analog scintillation record of equatorial stations Trivandrum-Tirunelveli, Pondicherry-Karur and Mumbai-Ujjain. The latitudinal extent of this belt is higher during d- and e-months compared with that of j-months. There is a positive correlation between the width of the belt and solar activity. Geomagnetic control on the width of the scintillation belt is studied from latitudinal variations of scintillation occurrence separately for geomagnetic quiet (Q), disturbed (D) and normal (N) days and also for the groups of days with low, medium and high Ap values (Fig. 8.18). It is observed from Table 8.2 that with increase in geomagnetic activity, width of the scintillation belt decreases.

Table 8.2 Belt variation with geomagnetic activity

Year	*Sunspot number*	*Q*	*D*	*N*	*Ap ≤ 5 Low*	*5<Ap≤ 20 Medium*	*A >20 High*
1991	144	15	11	13.5	15	12	11
1996	8	9.5	6.5	7	7	7.5	6

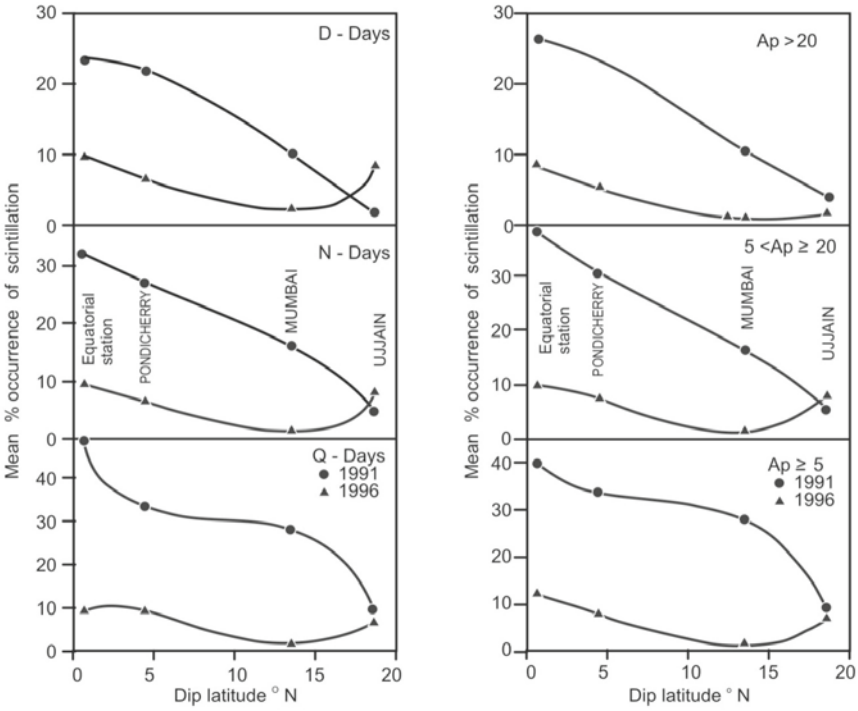

Figure 8.18. Scintillation belt variation as a function of geomagnetic activity recorded at different stations in 1991 and 1996.

II. Geomagnetic Pulsations

Geomagnetic pulsations or micropulsations are ultralow frequency (ULF) plasma waves in the Earth's magnetosphere. These waves have frequencies in the range 1 mHz to >10 Hz and appear more or less as regular oscillations in records of the geomagnetic field (Fig. 8.19). Geomagnetic oscillations or ULF pulsations as they are also called can be identified in electric field measurements in the ionosphere, magnetosphere and those made onboard spacecraft.

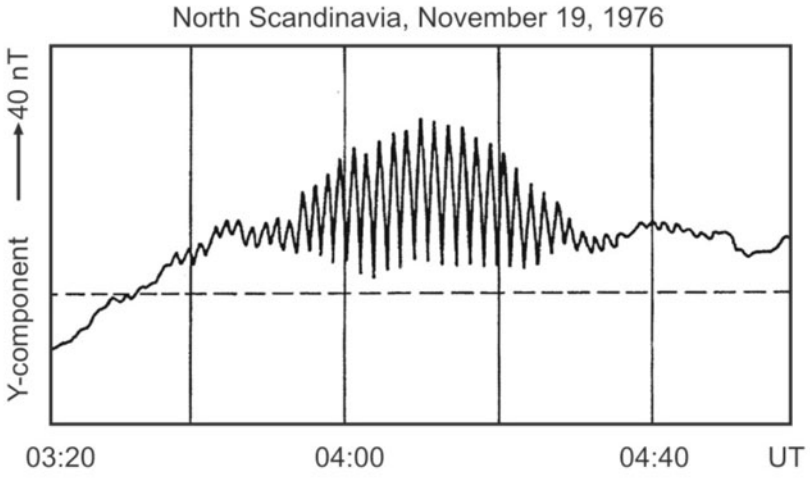

Figure 8.19. Geomagnetic pulsation of the Pc4 type, recorded at a magnetic observatory in North Scandinavia. The Y-component of the geomagnetic field is displayed relative to a quiet day period (Glaßmeier, 2007).

The lower frequency pulsations have wavelengths comparable to typical scale lengths of the entire magnetosphere. They are also interpreted as eigen oscillations of standing waves in the magnetospheric systems. The higher frequency waves are usually identifiable as proton ion-cyclotron waves in the magnetospheric plasma. The amplitudes of the lower frequency pulsations can reach several tens to hundreds of nT in the auroral zone while the higher frequency waves reach amplitudes of the order of a few nT.

Geomagnetic pulsations are classified into seven different types based on their oscillation period and appearance in magnetograms as almost continuous and more irregular pulsations (Table 8.3). The two classes, continuous pulsations (Pc) and irregular pulsations (Pi), are usually divided into subclasses. Micropulsation study is carried out to understand the mechanism by which they appear at low latitudes and also to know the speed and density of the solar wind and various characteristics of the ionized material present in the far away regions of space where EMF continues to retain its identity and exerts its influence in the magnetosphere. The study will provide clues to how the solar wind, the Earth's magnetosphere and its ionosphere are coupled with each

other on a global scale. These natural variations of the geomagnetic field can also be used for exploring the electrical conductivity distribution within the Earth to a depth of ~10 km.

Table 8.3 The IAGA classification of geomagnetic pulsations

Name	*Period range (sec)*
Continuous	
Pc1	0.2–5
Pc2	5–10
Pc3	10–45
Pc4	45–150
Pc5	150–600
Pc6 (during substorms this is known as Ps6)	>600
Irregular	
Pi1	1–40
Pi2	40–150
Pi3	>150

Some micropulsations seem to be caused by resonance of the field lines in response to Alfven waves with certain frequencies which are generated in the space environment even during quiet times. Examples of such pulsations from the Indian Antarctic station are shown in Fig. 8.20. Other pulsations notably Ps6 and irregular pulsations of the Pi type originate in the ionospheric and

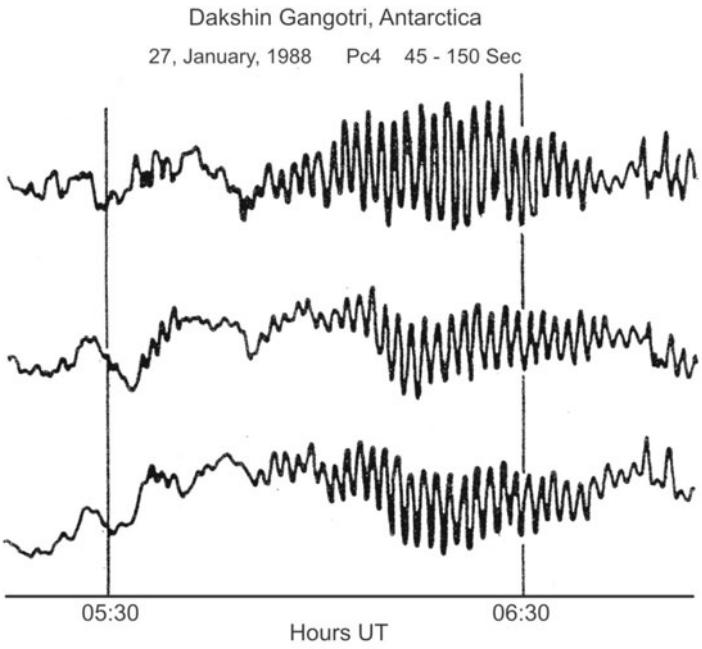

Figure 8.20. Pc4 magnetic pulsation seen on magnetic records from the Indian Antarctic station Dakshin Gangotri on 27 Jan 1988 (Rangarajan and Dhar, 1988).

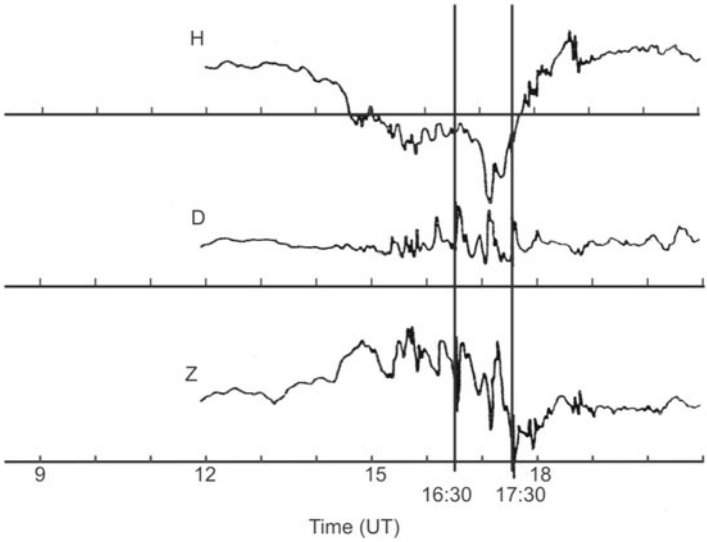

Figure 8.21. Ps6 pulsation event in the H, D and Z components of the geomagnetic field at auroral location Yellowknife on 16 Mar 1978 (Rajaram et al., 1990).

field aligned substorm currents which flow in the auroral regions during magnetically disturbed conditions. Shown in Fig. 8.21 is an example of the substorm associated Ps6 pulsation.

8.3 EQUATORIAL-LATITUDE ELECTRODYNAMICAL COUPLING AND ATMOSPHERIC STRUCTURE

The influence of geomagnetic activity is felt on the weather and climate. Though most of the currents associated with the geomagnetic field flow at altitudes far above the regions which control the weather, intriguing results have emerged from the studies of solar features, geomagnetic activity and meteorological parameters like the circulation patterns, temperature, drought conditions, rainfall, glaciations, etc. Scientists are working to identify a suitable catalyst that enables transfer of energy from the Sun and interplanetary space through the upper atmosphere to the lower regions. The mesosphere-stratosphere-troposphere (MST) radar facility at Tirupati in south India measures neutral winds (Table 8.1) and waves to high altitudes 80–10 km and even to 300–1000 km for studies of partial reflection radar (PRR).

I. Partial Reflection Radar

The partial radar (PR) operating in the medium frequencies (MF) yields useful information on mean winds, planetary waves, tides and gravity waves in thermosphere and lower atmosphere (60–100 km) region. The MF radar data provide quantitative information on the spaced antenna parameters, namely,

the fading time, the lifetime of the ground pattern, the pattern scale and pattern axial ratio.

The MF radar operating at Tirunelveli yields data on winds in the mesosphere and lower thermosphere in the altitude region (68–98 km) since 1992. Simultaneous data on geomagnetic field variation available from the nearby station, Trivandrum are made use to ascertain the range in the H component, which is a measure of the strength of the total ionospheric current flowing above the magnetic equator (Fig. 8.22a). The daytime (0700-1700 hrs) zonal winds between 84 and 98 km as determined by the MF radar for the days, 23 Dec and 26 Dec eastward winds are observed at all times except in the pre-noon hours at altitudes above 90 km (Fig. 8.22b). In the afternoon hours eastward wind speeds in excess of 20 m/sec are observed at an altitude of 88 km. On 26 Dec westward speeds exceeding 90 m/sec around noon at altitudes 96 and 98 km are noticed (Fig. 8.22c). In less than 6 km, the velocity is observed to change by more than 60 m/sec. Measurements on days with different electrodynamical conditions as noticed in the ground geomagnetic field variation indicate the influence of the equatorial current on the drifts measured by partial reflection MF radar.

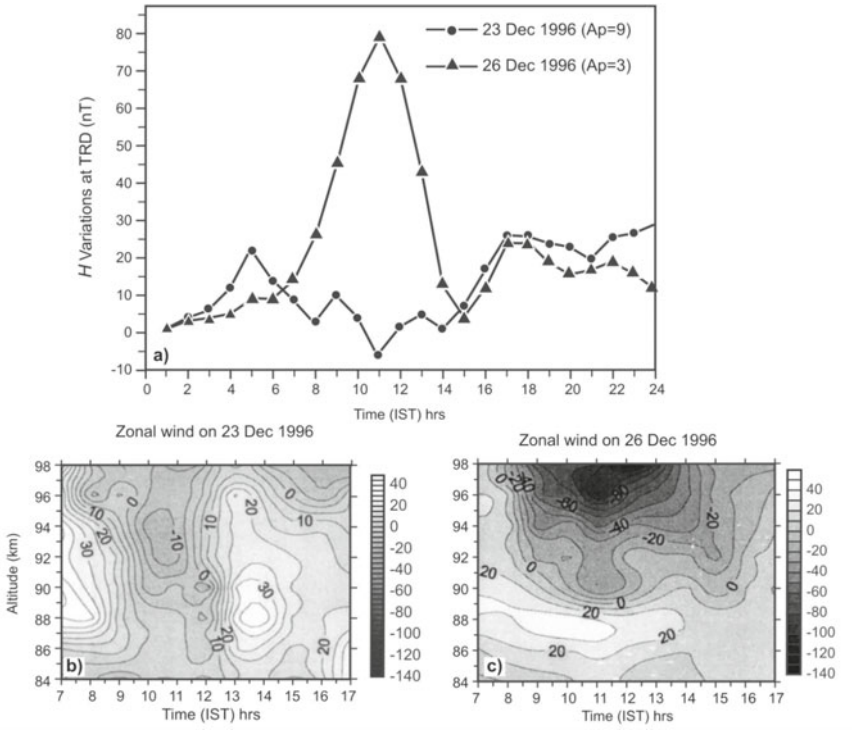

Figure 8.22. (a) Temporal variation of the horizontal component of the geomagnetic field as measured on ground at the equatorial station, Trivandrum (TRD), on 23 and 26 Dec 1996. (b, c) Daytime (0700-1700) radar zonal winds between 84 and 98 km on two days 23 December and 26 December 1996 (Gurubaran and Rajaram, 2001).

Further, PR data revealed a relationship between the tidal characteristics and the occurrence of afternoon CEJ. A clear anti-correlation is seen between the afternoon electrojet strength and amplitude of semi-diurnal tide in solstitial months of June and July 1995. It also revealed the presence of 3.5-day ultra-fast Kelvin (UFK) wave in mesopause region, at 84–98 km. Also, medium frequency radar observations of 3.5-day UFK wave in 84–98 km mesopause region over Tirunelveli for a period of ~3 years are monitored, wherein the UFK wave revealed semi-annual variability at heights (~85 km) where the mesopause semi-annual oscillation in the mean wind peaks. Large-amplitude wave events preferentially occur during westward flow regimes of the background wind. Mean eastward winds and their shears are qualitatively shown to be associated with bursts of waves with moderate amplitudes. Vertical wavelength estimates agree with earlier estimates based on satellite temperature retrievals for a wave number 1 UFK wave.

II. Airglow Experiments

Airglow measurements are complementary to the partial reflection radar since it yields mesospheric rotational temperatures at ~85 km during moonless clear nights. The mesopause region acts as an interface between the mesosphere and the lower thermosphere. It also represents the transition zone dominated by photochemical processes (lower atmosphere) and transport processes (upper atmosphere). One of the manifestations of this sort of transitional character is the multiple airglow emitting layers situated close to one another. The three most important airglow emissions from the mesosphere are: (1) vibrational rotational bands of hydroxyl radical (OH), (2) atomic and molecular oxygen emissions and (3) emissions from metallic atoms like sodium, magnesium, etc. The main energy source is the solar UV radiation, which dissociates the molecular oxygen into atomic oxygen, which in turn becomes chemically active. Transport effects enable the downward flux of O towards mesopause where O_3, OH and active O_2 are formed.

The technique uses measurement of the relative intensities of rotational lines in the hydroxyl vibration rotation band at wavelengths of 733.7 and 740.2 nm using tilted filter assembly. The tilting filters enable correction for background levels and provision is made for three additional filters that can be used for other wavelengths like 630 nm, 557.7 nm and 589.6 nm so that wave dynamical processes that modulate airglow intensities at different heights can be studied. The optical photometer is used to study crucial problems dealing with dynamical heating of the mesopause region through planetary waves, tides and gravity waves. By monitoring airglow emissions from the ground, a variety of quantitative information regarding chemical composition, wind velocity and temperature of the upper atmosphere during quiet and disturbed period is gained.

i. Mesosphere thermodynamics: Temperature of the mesosphere is an important physical parameter in remote sensing investigations of the mesopause thermodynamics and chemistry. At these latitudes, due to chemical reactions in atmospheric constituents, airglow emissions are produced. These emissions, if measured from ground-based instruments, infer the photochemistry and dynamics of the respective regions. Simultaneous measurements of several airglow emission lines from mesopause region provide important information related to the propagation of gravity waves, since these emission layers are situated between 80 and 100 km.

Measurements of hydroxyl rotational temperature for the (8,3) Meinel band are reported from observations of the ratio of relative intensities of $P_1(2)$ and $P_1(4)$ lines of the OH (8,3) band at Kolhapur (16.8°N, 74.2°E, dip lat 10.6°N) during the period 1 Nov 2002 to 29 April 2003 using tilting-filter photometers. Mean values of rotational temperature are computed for 60 nights. The monthly mean value of temperature lies in the range 194±11 to 208±18K. The mean rotational temperature obtained from all the measurements is found to be 202±15K. The results agree with other low latitude measurements of rotational temperature using photometric airglow techniques. Quasi-periodic fluctuations with ~1 to 2 hrs period are prominent on many nights. Furthermore, the results show a general agreement between observations and model (MSIS-86) predictions.

ii. Monitoring of gravity waves using all-sky imager: With the development of cooled charge-couple device (CCD) detector, it is possible to detect spatial and temporal variation of small-scale structures in airglow emissions more accurately. The night airglow observations were carried out from Kolhapur and Panhala (17.0°N, 74.2°E; height above msl 3200 ft) during Jan and Feb 2001, using tilting-filter photometers (630 nm and OH) and a CCD based multi channel all-sky imager, respectively, on clear and moonless nights. The multi-wavelength airglow imaging enables to study horizontal structures of small-scale gravity waves at various heights in the region of emissions and to investigate propagation of those waves in detail. Hydroxyl and OI 557.7 nm images on the night of 18 Feb 2001 showed row-like structures moving from north to south direction spanning over 500 km in the sky. The observed horizontal phase speed of ~50 m/sec, wavelength ~25 km and wave period of ~8 min of the atmospheric gravity waves were determined from a set of sequential images of OI 557.7 nm at 97 km and OH at 86 km observed at Panhala (Fig. 8.23). These are the first observation of the signature of atmospheric gravity waves using an all-sky imager in Indian region showing perturbation in density in the 80 to 100 km mesospheric region. Signatures of gravity waves are also seen at Kolhapur (Fig. 8.24).

Monochromatic imaging of large scale F-region plasma depletions associated with equatorial bubbles present during ESF occurrence shows simultaneous signature of depletions observed in OI 630 nm, OI 557.7 nm and

OI 777.4 nm. Also, the signature of midnight temperature maximum in OI 630 nm airglow is seen. An all-sky image (Fig. 8.24) depicts intense enhancement in OI 630 nm intensity on the night of 7 Feb 2000 ~23:45 hrs during the main phase of magnetic storm with minimum geomagnetic activity index D_{st} reaching at –41 nT.

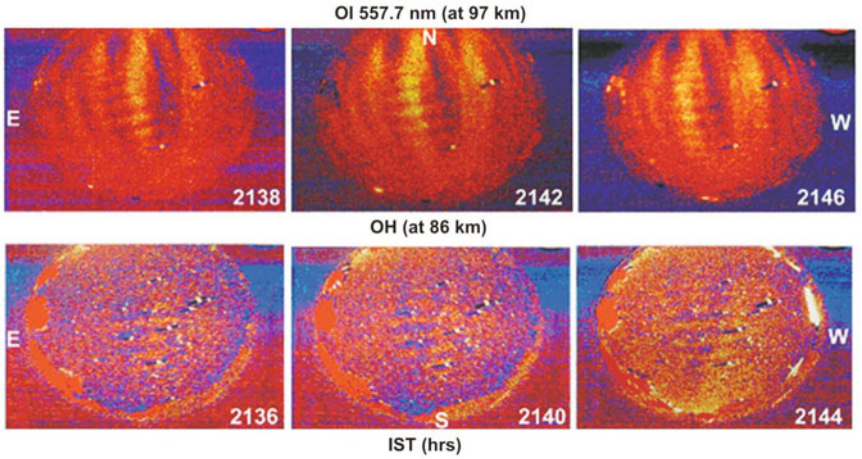

Figure 8.23. Signature of gravity waves observed by an all-sky imager at Panhala on 18 February 2001 (Mukherjee, 2003a,b).

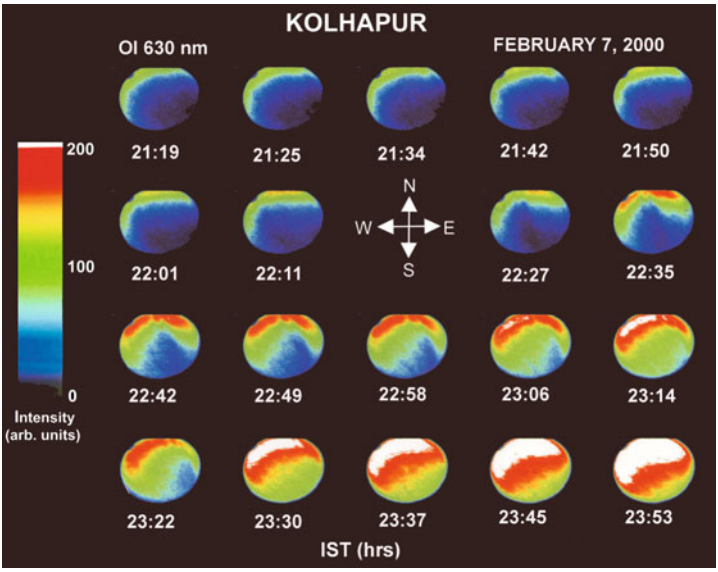

Figure 8.24. Signature of gravity waves observed by all-sky imager at Kolhapur on 7 February 2000 (Mukherjee, 2003a,b).

8.4 ANTARCTIC MAGNETIC DATA

To establish its place in the global arena, Indian scientists are carrying out a number of diverse experiments in Antarctica. India has been launching scientific expeditions to the Antarctic continent since 1981 and has permanent magnetic stations at Maitri and Dakshin Gangotri. The stations at Maitri and Dakshin Gangotri, where the experiments are conducted, are at latitude 70°S and longitude 12°E. Magnetic experiments are carried out to: (1) study the magnetospheric influences on terrestrial magnetic field in the continent on a long-term basis and to carry out systematic magnetic field variation, (2) establish a link between the magnetic field variation in the polar and equatorial regions, and (3) examine subsequently the subsurface structures of the continent using magnetic field variations.

The magnetic field in the polar region gets directly connected to the IMF and solar wind fluctuations, which are most easily communicated to these regions. The diurnal variations in the magnetic field in the polar regions are used to monitor the sector polarity of the IMF. At the same time, sector polarity effects are discernable in low latitude magnetic field variations. Thus the equatorial and polar magnetic field variations can be correlated or studied in tandem for similar features. Also, since the fluctuations in the interplanetary medium are communicated to the auroral ionosphere, these can be stored in the magnetic records.

Direct deposition of solar wind energy occurs at latitudes exceeding 60° geomagnetic latitudes, i.e. auroral and higher latitudes. The lower latitudes, however, are shielded from such direct energy deposition by the closed magnetic field configuration. It is the higher latitudes too, which experience the direct effect of the Earth's geomagnetic response to changes in the direction of the solar magnetic field (the IMF) from northward to southward and vice versa.

The magnetic field variations are also used in natural resource exploration. The rapidly dwindling resources of other oceanic and continental landmasses necessitate delineation of these prized resources on the Antarctic continent, though any exploitation of such resources is banned through many international treaties. However, such probing is also important in understanding the geological history of the Indian subcontinent. India broke away from the Antarctic continent only about a hundred million years ago. Thus, the two have a shared geological history, which can be unearthed by depth sounding along relevant coasts and interior of the two continents. Initially only the total magnetic field was measured using a PPM, but later on till 1989, a single-station fluxgate magnetometer recorded variations in X, Y and Z components.

I. Geomagnetic Studies at Antarctica

The MO at Maitri yields information on physical processes at work in the distant magnetospheric regions. Daily variations and pulsations (Pc2 and above) in the X, Y and Z components at the stations show time lags. These are used to

derive the velocity and direction of the auroral current systems. Magnetograms from the Maitri are used to understand the dependence of HF radio communication on the electromagnetic state of the Earth's ionosphere-magnetosphere system. Also the local time and seasonal variations of the Pc3, Pc4, Pc5 and Pc6 pulsations are studied.

II. Secular Variation Studies at Antarctica

The secular variation of the internal geomagnetic field at Maitri is currently causing a very rapid drop in total field F (~120–150 nT/yr), and at the south magnetic pole (~50 nT/yr). Specifically, studies on the characteristics of secular variation in total F at Antarctica for the interval 1960-1995 are carried out using contour plots of magnetic field variations. The period under investigation is grouped into 5-yr intervals and the average field magnitudes were computed and studied for each of these 5-yr zones (Fig. 8.25). The characteristics of average dipole, quadrupole and octupole fields are determined and their contribution to the total field variation is studied.

Antarctica shows absence of westward drift, which is a prominent feature of secular variation at some other locations. A region of peak decrease in total F lying in the Antarctic region is seen to be stationary. The rate of decrease of this feature is in the vicinity of ~100 nT/yr and the magnitude of this decrease is itself falling since 1980. The dipole field variation contributes less than 40% to this feature and the quadrupole and octupole fields contribute to an increasing

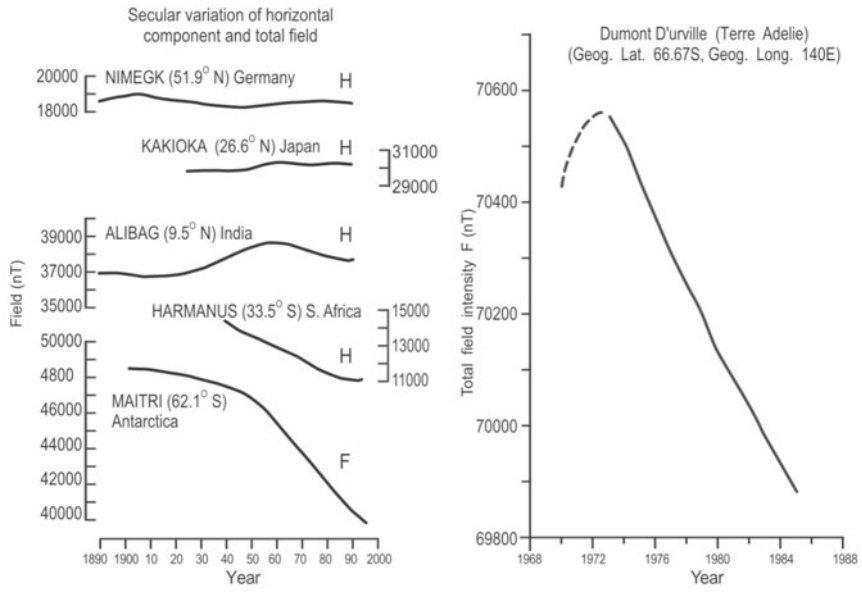

Figure 8.25. Secular variation changes observed at Antarctica and different places over the globe.

field in this region. This implies that a large geomagnetic contribution comes from localized region. Recent studies of secular variation at the core-mantle boundary have postulated that flux expulsion resulting from fluid upwellings could be a cause of secular variation features in the southern hemisphere high latitudes. The northern hemisphere also has a long-lived region of decreasing total magnetic field, but this is located at the mid latitudes. This northern hemisphere feature has a significant contribution from the decreasing dipole field.

III. Magnetic and Atmospheric Measurements

Monitoring the changes in the geomagnetic field on a continuous basis yields information on the electromagnetic state of the near and far space environment of the Earth. Magnetic recordings are a comparatively inexpensive method to monitor the signatures associated with large-scale currents generated in the ionosphere and magnetosphere.

The atmospheric global electricity is provided by a difference in electrical potential (~300 kv) between the highly conducting ionosphere and the Earth's surface, with the total current flow between the two of $\sim 10^6$ A. The air-Earth current is one component that links electric fields and currents flowing in the lower troposphere, ionosphere and magnetosphere and is part of a giant global electrical circuit. The integrated approach provides a good framework for exploring inter-connections and coupling of various regions of the atmosphere and also for explaining the solar-terrestrial relationship. The results from such studies will generate relationships between climate and solar sunspot cycle, and also between solar wind and short-term weather changes.

Ground-based measurements of electrical parameters pose difficulties in interpreting them in terms of the global air-Earth current since they are essentially the superposition of currents from various sources, namely, conduction current linked to the existence of vertical electric field, convection current density, diffusion current due to the movement of charged particles, lightning current due to rapid lightning over the measuring site and precipitation current associated with showers. The sum of these currents is called the Maxwell current. Different types of sensors are used for the measurement of air-Earth current like Wilson plate, spherical sensors, and the horizontal long wire antenna. Magnetometer and riometer data in both analog and digital form exists for the study of a wide spectrum of polar geomagnetic problems.

Air-Earth Maxwell currents and atmospheric electric fields, which require very clean conditions free from anthropogenic pollution, are measured at Antarctica to study the global electrical circuit. It extends the understanding of magnetosphere-ionosphere electrical coupling to the troposphere, an area most important because of its relevance to solar-weather relations. Figure 8.26 depicts Maxwell current density for a selected fair-weather day in the month of Feb 2002 observed at Maitri.

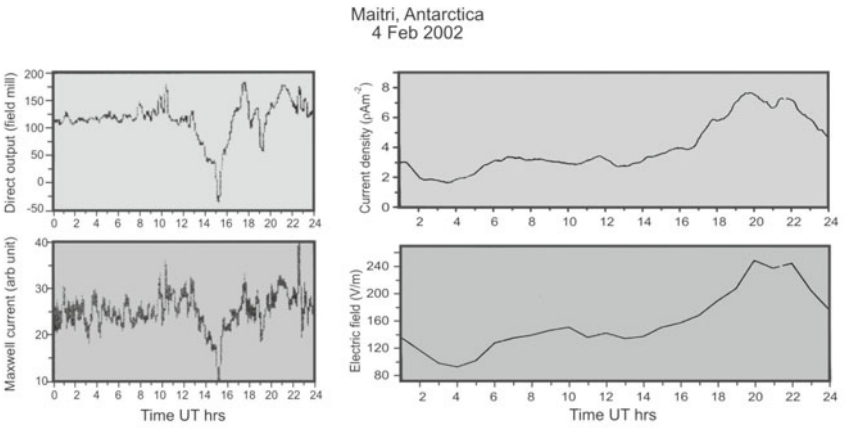

Figure 8.26. Air-Earth Maxwell currents observed at Maitri, Antarctica.

IV. Crustal Magnetic Anomalies

Studies of subsurface electrical conductivity and magnetic susceptibility from the Antarctic data are a little difficult because the inducing source field of the auroral electrojet is a sharply-bounded, non-uniform one. In the early years, a PPM was used to carry out a ground magnetic survey along six profiles, each 10–15 km long. Contours obtained of the magnetic field values show a pronounced magnetic low in the vicinity of the Indian Antarctic locations with axis in the N-S direction; and this is interpreted as the continuation of a rift valley below the ice-shelf.